Agrawal, A., Kejalakshmy, N., Uthman, M., Rahman, B. M., Kumar, A. & Grattan, K. T. (2012). Ultra low bending loss equiangular spiral photonic crystal fibers in the terahertz regime. AIP Advances, 2, doi: 10.1063/1.4726055 <http://dx.doi.org/10.1063/1.4726055>

Ultra low bending loss equiangular spiral photonic crystal fibers in the terahertz regime

Arti Agrawal, N. Kejalakshmy, M. Uthman, B. M. A. Rahman, A. Kumar et al.

Citation: AIP Advances **2**, 022140 (2012); doi: 10.1063/1.4726055

View online: http://dx.doi.org/10.1063/1.4726055

View Table of Contents: http://aipadvances.aip.org/resource/1/AAIDBI/v2/i2

Published by the American Institute of Physics.

Ultra low bending loss equiangular spiral photonic crystal fibers in the terahertz regime

Arti Agrawal,[1,a] N. Kejalakshmy,[1] M. Uthman,[1] B. M. A. Rahman,[1] A. Kumar,[2] and K. T. V. Grattan[1]
[1]*School of Engineering and Mathematical Sciences, City University London, Northampton Square, London, EC1V 0HB, United Kingdom*
[2]*Department of Physics, Indian Institute of Technology Delhi, New Delhi, 110016, India*

(Received 26 October 2011; accepted 2 May 2012; published online 4 June 2012)

An Equiangular Spiral Photonic Crystal Fiber (ES-PCF) design in Topas® for use in the Terahertz regime is presented. The design shows ultra low bending loss and very low confinement loss compared to conventional Hexagonal PCF (H-PCF). The ES-PCF has excellent modal confinement properties, together with several parameters to allow the optimization of the performance over a range of important characteristics. A full vector Finite Element simulation has been used to characterize the design which can be fabricated by a range of techniques including extrusion and drilling. [http://dx.doi.org/10.1063/1.4726055]

Probes for use in the Terahertz (THz) regime can be applied in security-sensitive areas such as monitoring drugs, explosives or weapons in a non-destructive manner and in achieving a better understanding of the dynamics of complex biological systems.[1] This has led to a concerted research effort in the area of THz sources, detectors and waveguides and for the successful implementation of THz systems, low loss and commercially viable waveguides are essential.

Plastic,[2] metallic ribbon[3] waveguides and polymer PCF[4,5] have demonstrated THz guidance. The latter often utilize a 'drill and draw'[5,6] or 'stack and fuse'[4] technology in their fabrication. Recently, very low loss operation in a PCF made from Topas® polymer has been demonstrated[5] and a new class of porous fibers have also been reported,[7–9] though achieving high porosity is not trivial.[9] In this letter, an Equiangular Spiral (ES) PCF design inspired by nature[10,11] in Topas® is presented for THz frequencies. This ES-PCF can show significantly better performance over loss compared to the conventional Hexagonal PCF (H-PCF). An **H**-field based full vectorial Finite Element Method (FEM)[12] along with conformal transformations[13] has been used for the rigorous analysis of the fibers.

Spiral curves appear in plant and animal life forms as well as huge structures such as galaxies. The ES-PCF design presented here is adapted from the original design reported previously by the authors.[10,11] A schematic of the ES-PCF is shown in Fig. 1(a). Each arm of air holes, (depicted by air holes of same colour in Fig. 1(a); air hole radius, r) forms a single ES of radius r_o, and angular increment θ, given by the polar equation:

$$r_{spiral} = r_o.e^{\theta \cot \alpha} \tag{1}$$

$$\alpha = \frac{(n-2)\,\pi}{2n} \tag{2}$$

Where α is the constant angle between a radius of the equiangular spiral and the tangent at the end point of the radius and r_{spiral} is the distance at any point along the spiral arm from the centre

[a]Author to whom correspondence should be addressed. Electronic mail: arti.agrawal.1@city.ac.uk

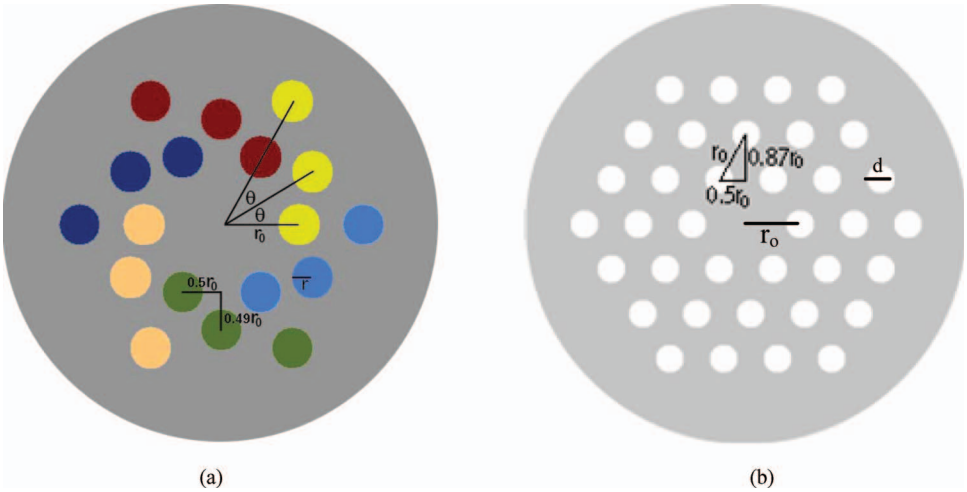

FIG. 1. (a) Schematic of the ES-PCF structure. (b) Schematic of the H-PCF structure.

of the structure. Each air-hole is separated by an angular increment of θ with respect to the previous/successive air hole in the same arm. The total number of air holes in each arm represents the number of rings in the ES-PCF and the total number of air holes is thus simply the product of the number of arms with the number of rings. The *x,y* coordinates of the centre of each air-hole can be found from Equation (1). The ES-PCF structure shown in Fig. 1(a) has 6 arms and 3 rings with θ=*30*° to ease comparison of the structure with that of the conventional H-PCF (shown in Fig. 1(b)).

The H-PCF has an hexagonal air hole arrangement in which the separation between air holes is constant and is also equal to the distance from the centre of the structure to the centre of the air holes in the first ring (it is normally termed Λ, and in this paper to aid comparison with the ES-PCF we set $\Lambda=r_o$). The diameter of the air holes is also fixed and equal to *d*. The optical properties of the H-PCF are determined chiefly by the d/Λ ratio. While in the ES-PCF it has been found possible to tune the modal characteristics of the field in the ES-PCF by choosing a suitable combination of values for the fiber parameters: the number of arms (n), θ (spiral angle), r_o, (spiral radius), r,(air hole radius), and the number of rings.

A key characteristic for THz waveguides is the Modal Loss (ML), which is the sum of the Confinement Loss (CL), the Bending Loss (BL) and the Material Loss (MaL) associated with the mode. A comparison of the ML in the H-PCF (the LMA design),[5] and a ES-PCF (optimized with the same number (36) of air holes as the LMA) is presented where the key fiber parameters used are as follows – for the LMA: Λ=560μm, r=125μm, d/Λ=0.45 and for the ES-PCF: 7 arms, 5 rings, r_o=560μm, r=250μm, θ=*27*°.

Figure 2 shows the ML and the normalized spot size variation with the bend radius. To separate out the effect of the air-hole arrangement, this initial result assumes a loss less material, although MaL is included in later results. From Fig. 2 it can be seen that for large bend radii (100-10000*mm*), the loss is primarily CL and the ES-PCF loss is about three orders of magnitude lower than for the H-PCF. For bending radii lower than 100*mm* (where CL and BL are present), the H-PCF suffers severe mode leakage while the mode is extremely well confined in the ES-PCF with loss lower by 5-6 orders of magnitude. The spotsizes of the guided modes are similar in both fibers over this entire range.

We explain here the mechanism for the lower bending loss in the ES-PCF. The bending of a PCF leads to the distortion of the optical mode which loses its shape and tends to move towards regions of higher equivalent refractive index.[13–15] In the ES-PCF the bridge regions of high refractive index between air holes are much smaller and narrower than in the H-PCF (distance of the air holes in the second ring from the first ring is 0.49 r_o in the ES-PCF while it is 0.87 r_o in the H-PCF - see Figures 1(a) and 1(b)). By choosing an appropriate value of θ, the placement of air holes in the second ring block the spread of the field into the polymer regions between the holes. This can be

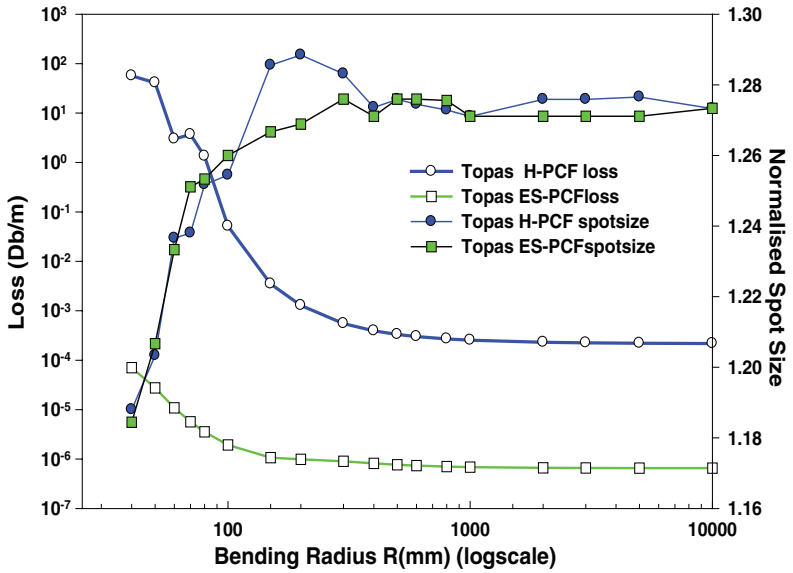

FIG. 2. Modal loss (ML) and normalized spot size variation with bend radius for the H-PCF and ES-PCF.

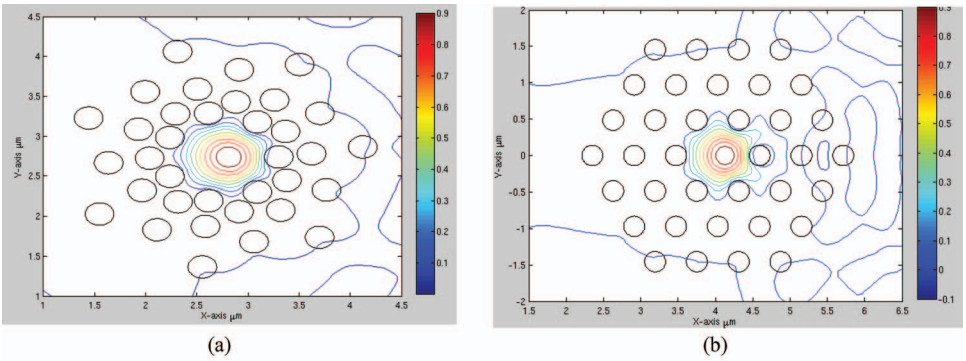

FIG. 3. (a) Field profile in the bent ES-PCF, where bend radius=60*mm*. (b) Field profile in the bent H-PCF, where bend radius=60*mm*.

seen clearly in Fig. 3(a) which shows the fundamental mode in the bent ES-PCF (to show the effect of the air holes, the air holes are also drawn in the figure). A similar behavior is observed in Teflon PCF (but not shown here). This is the main cause that even when the fiber is bent, in the ES-PCF the field is blocked from spreading out of the core by the second ring of air holes. In the H-PCF the distance between the first and second ring air holes is large enough to allow the field to escape from the core through this bridge especially when bent, as can be seen clearly in Fig. 3(b).

When the addition of MaL is considered (see Fig. 4), there is a marked increase in the ML values due to the modal field residing mostly in the solid polymer core and the MaL dominating. The ML shows a sharp increase as the bend radius decreases below 10 *cm* for the H-PCF (LMA) design, while for the ES-PCF it remains almost constant. Bend loss is the dominant loss mechanism for such small bend radii; the ES-PCF does not allow the modal field to escape into the cladding in a way similar to the H-PCF (see Figs. 5(a) and 5(b)) or oscillation in the BL due to mode degeneration).[14] Thus, for applications where fibers may need to be wound on tight spools, the ES-PCF can show the better loss performance (BL ∼10dB/cm even for very tight bends ∼ 2 cm). At large bend radii (where the loss is primarily due to MaL and CL) the loss values are almost similar for both PCF designs. Even when examining the CL variation with frequency for straight fibers, both PCFs exhibit

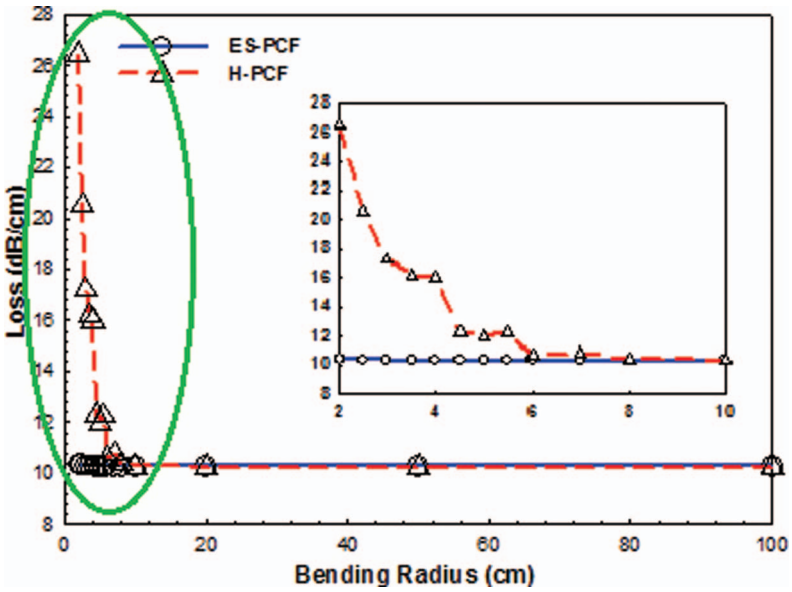

FIG. 4. Modal loss (including material loss) variation with bend radius at 1THz for the H-PCF and ES-PCF.

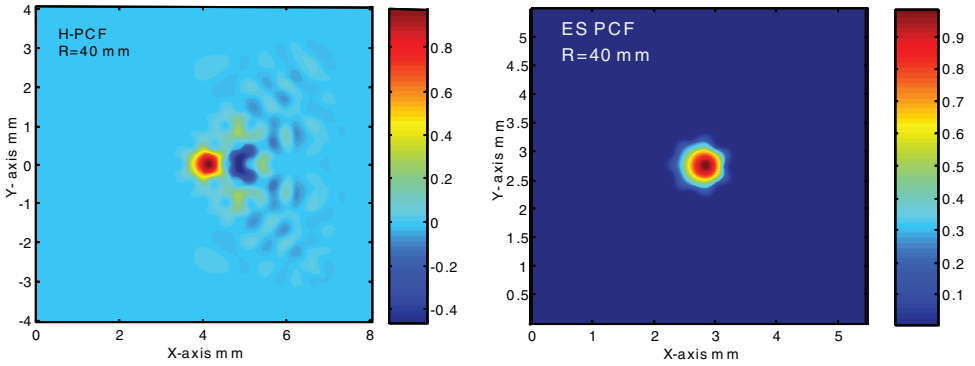

(a) Hexagonal PCF (b) Equiangular Spiral PCF

FIG. 5. Field profile of the fundamental mode in the bent Hexagonal PCF (mode leaking into cladding region) and the ES PCF with bend radius 40*mm*.

almost similar performance (not shown here). Therefore, for a modest value of d/Λ the ES-PCF shows a better overall modal confinement than does the H-PCF.

Porous fibers on the other hand have much lower ML than PCF since an appreciable portion of the field is in the air holes. However, besides the loss, other modal properties of the porous fibers and ES-PCF are different. The normalized spotsize (see Fig. 6) and power confinement factor in the cladding (inset of Fig. 6) are compared as a function of frequency for the ES-PCF, H-PCF and porous fiber, all simulated in Teflon. The parameters of the porous fiber are taken from the literature.[8] For the H and ES-PCF, the normalized spotsize is small and rises only when frequency decreases below 0.4 THz (approaching cut off).[16] In the case of porous fibers, the cut-off region starts when f≈0.8 THz and thus the operating bandwidth of the porous fibers may not be as large as that of ES-PCF. In addition, the power confinement factor (the percentage of optical power in the cladding) at 1 THz is as low as ∼0.8% for the H-PCF and ES-PCF, while it is ∼40% for the porous fiber with d/Λ=*0.9*, 50 times higher than of the two PCFs. This implies that there could be power loss unless these fibers are suspended in air as well as susceptibility to the surrounding environment.

In conclusion, an ES-PCF design has been presented which has shown the ability for very effective control of the modal field – in some cases better than the hexagonal design and thus

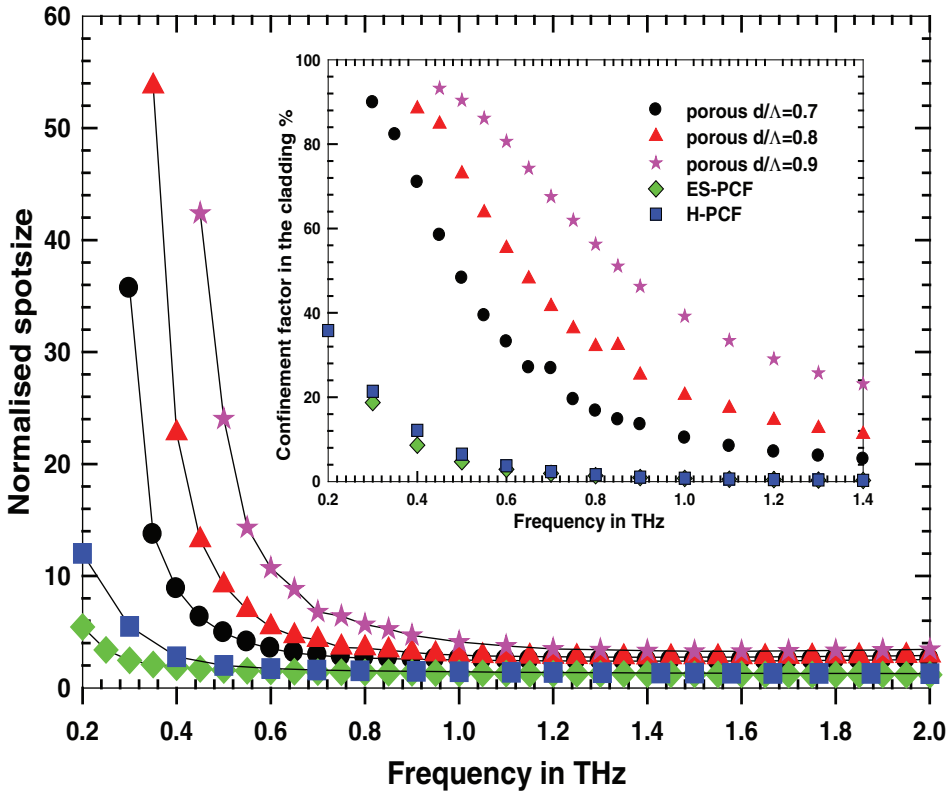

FIG. 6. Normalized spotsize variation with frequency for the porous fiber, the H-PCF and ES-PCF in Teflon.

allowing significantly lower bend loss. Further, the operating bandwidth of the ES-PCF can be larger than in porous fibers. The fabrication of the ES-PCF should be possible using the extrusion and/or drilling and is not beyond present capabilities or more challenging than for other designs.

[1] W. L. Chan, J. Deibel, and D. M. Mittleman, Rep. Prog. Phys. **70**, 1325 (2007).
[2] R. Mendis and D. Grischkowsky, J. Appl. Phys. **88**, 4449 (2000).
[3] K. Wang and D. M. Mittleman, Nature **432**, 376 (2004).
[4] M. Goto, A. Quema, H. Takahahi, S. Ono, and N. Sarukura, Jpn. J. Appl. Phys, Part 2 **43**, L317 (2004).
[5] K. Nielsen, H. K. Rasmussen, A. J. L. Adam, P. C. Planken, O. Bang, and P. U. Jepsen, Opt. Express **17**, 8592 (2009).
[6] M. A. van Eijkelenborg, M. C. J. Large, A. Argyros, J. Zagari, S. Manos, N. A. Issa, I. Bassett, S. Fleming, R. C. McPhedran, C. Martijn de Sterke, and N. A. P. Nicorovici, Opt. Express **9**, 319 (2001).
[7] A. Hassani, A. Dupuis, and M. Skorobogatiy, App. Phys. Lett. **92**, 071101 (2008).
[8] S. Atakarmians, S. Afshar Vahid, B. M. Fischer, D. Abbott, and T. M. Monro, Opt. Express **16**, 8845 (2008).
[9] A. Dupuis, J.-F. Allard, D. Morris, K. Stoeffler, C. Dubois, and M. Skorobogatiy, Opt. Express **17**, 8012 (2009).
[10] A. Agrawal, N. Kejalakshmy, B. M. A. Rahman, and K. T. V. Grattan, IEEE Photon. Tech. Lett. **21**, 1722 (2009).
[11] A. Agrawal, N. Kejalakshmy, M. Uthman, B. M. A. Rahman, and K. T. V. Grattan, in *CLEO:2011 Laser Applications to Photonic Applications*, (Optical Society of America, Baltimore, 2011S) paper CThN1.
[12] B. M. A. Rahman and J. B. Davies, J. Lightwave Technol. **2**, 682 (1984).
[13] M. Heiblum and J. H. Harris, IEEE J. Quantum Electron. **QE-11**, 75 (1975).
[14] B. M. A. Rahman, N. Kejalakshmy, M. Uthman, A. Agrawal, T. Wongcharoen, and K. T. V. Grattan, App. Opt. **48**, G131 (2009).
[15] B. M. A. Rahman, M. Uthman, N. Kejalakshmy, A. Agrawal, and K. T. V. Grattan, App. Opt. **50**, 6505 (2011).
[16] N. A. Mortensen, Opt. Express **10**, 341 (2002).